TELKOMNIKA Telecommunication, Computing, Electronics and Control
Vol. 18, No. 6, December 2020, pp. 2868~2877
ISSN: 1693-6930, accredited First Grade by Kemenristekdikti, Decree No: 21/E/KPT/2018
DOI: 10.12928/TELKOMNIKA.v18i6.16119

A miniaturized printed UWB antenna with dual notching for X-band and aeronautical radio navigation applications

Mohammad Ahmad Salamin[1], Sudipta Das[2], B. T. P. Madhav[3], Soufian Lakrit[4], Avisankar Roy[5], Asmaa Zugari[6]
[1]Electrical, Communication, and Electronics Engineering, Palestine Polytechnic University, Palestine
[2]Department of Electronics and Communication Engineering, IMPS College of Engineering and Technology, India
[3]Department of Electronics and Communication Engineering, Koneru Lakshmaiah Education Foundation, India
[4]Smart Communications Research Team, EMI, Mohammed V University, Morocco
[5]Department of Electronics and Communication Engineering, Haldia Institute of Technology, India
[6]Information and Telecommunication system Laboratory, Facility of Sciences, Abdelmalek Essaâdi University, Morocco

Article Info

Article history:

Received Mar 22, 2020
Revised Jun 26, 2020
Accepted Jul 9, 2020

Keywords:

ARN band
Microstrip antenna
Monopole antenna
Notched band
UWB applications
X-band

ABSTRACT

A low cost miniaturized ultra-wideband (UWB) microstrip antenna with dual notched band for X band and aeronautical radio navigation (ARN) is presented in this article. The antenna (19×25 mm^2) is composed of a half-circular ring as a radiation patch with an incomplete ground plane. The measured results indicate a fractional bandwidth of 112% for $S_{11} \leq -10$dB between 3 to 10.6 GHz. The dual notched band has been achieved by incorporating window shaped microstrip closed ring resonators at the rear surface of the designed structure. The first notch band is centered at 7.5 GHz (7-8.1 GHz) to reject interference with X-band downlink (7.25 to 7.74 GHz) and second band centered at 9.1 GHz (8.6-9.4 GHz) to reject interference with ARN (8.7 to 9.2 GHz). The simulated and measured return loss, radiation pattern, and gain shows good agreement which confirms the applicability of the designed antenna for the intended UWB applications.

Corresponding Author:

B. T. P. Madhav,
Department of Electronics & Communication Engineering,
Koneru Lakshmaiah Education Foundation,
Green Fields, Vaddeswaram, Andra Pradesh-522502, India.
Email: btpmadhav@kluniversity.in

1. INTRODUCTION

After early 1888, when Heinrich Hertz (1857-1894) proved the presence of radio waves, the antenna becomes a portion of electrical appliances in the wireless communication scheme [1]. In 2002, the Federal Communication Commission (FCC) sanctioned the unlicensed band (3.1 to 10.6 GHz) for the operation of ultra-wideband (UWB) systems [2]. Since then, UWB technology has become very attractive and promising for modern wireless communication applications due to its wideband characteristics. This issue has inspired the researchers of the antenna community for the design and development of efficient UWB antennas. Microstrip antennas have become very popular owing to their appealing light weight, compact size, low profile, and simple manufacturing characteristics [3-5]. Recently many researchers have carried out investigations on microstrip antennas for achieving wideband operation by implementing etched substrate mechanism [6] and connected square-shaped open-loop resonator [7]. Multiband configurations can be achieved by employing a slotted patch [8], defected ground plane [9], and parasitic open-loop ring resonators [10, 11]. Similarly,

the researchers have proposed a variety of printed monopole antennas for UWB application [12-19]. However, the presence of some other narrow dedicated coexisting bands within the UWB spectrum is a serious threat as it interferes with UWB systems and degrades the performance of it. So, the researchers of antenna community have expressed intensive interest on designing UWB antennas with band rejection capabilities to remove undesired interference from existing narrowband wireless systems such as worldwide interoperability for microwave access (Wi-MAX) from 3.3 to 3.9 GHz, wireless local area network (WLAN) from 5.15 to 5.825 GHz and X-band satellite communication from 7.25 to 8.4 GHz (downlink: 7.25-7.745 GHz, uplink: 7.9-8.4 GHz) which creates interference with UWB system. Different methods for incorporating band-notched features in wideband antennas have been introduced, involving parasitic resonator [20], a combination of slot loaded patch and coplanar waveguide (CPW) feeding [21], elliptical radiator with slot loaded ground plane [22], shared radiator [23], stub loading [24], etching overlapped U shaped and C-shaped slot [25], maple leaf-shaped monopole [26], a combination of M-shaped slot and C-shaped strip [27], electromagnetic band gap (EBG) resonator [28], CPW fed split ring resonator [29], crossed shaped slot-loading [30], tapered radiating element [31], strip loading [32], fractal monopole with trapezoidal rings [33], and split ring resonator [34]. But many of the reported UWB antennas (except [31]) were designed to create notch function for WLAN and/or Wi-MAX application bands.

This paper is also associated with the design and realization of monopole microstrip UWB antenna with band rejection features and the model intended is distinct from the methods reported in the literature [20-34]. We aim is to create dual notch bands to suppress the interference of X band (downlink) and aeronautical navigation (AN) with the UWB systems. The dual band notches have been achieved using window shaped microstrip closed ring resonators which are embedded on the ground plane of the monopole antenna. The first notched frequency band (7-8.1 GHz) is capable to mitigate the interference from the X-band downlink communication system (7.25-7.74 GHz). The second notch band (8.6-9.4 GHz) can be used to prevent interference from aeronautical radio navigation (8.7-9.2 GHz). The proposed antenna supports the UWB application band in a compact size and with higher gain compared to the notched band UWB antennas reported in [20-33]. The advantages of the proposed antenna are compact dimension, improved gain, good impedance matching, suitability for wideband communication systems, and multi-band filtering capability to eliminate the interference of existing communication systems (X-band downlink and aeronautical radio navigation) with the UWB systems. Moreover, the nearly Omni-directional radiation characteristics at the H plane across the operating band of frequencies makes the suggested antenna a preferable choice for ultra-wideband (UWB) devices.

2. ANTENNA DESIGN

The design layout of the proposed antenna is depicted in Figure 1. The proposed structure is designed by employing a low cost 1.6 mm thick FR-4 material with a relative permittivity of 4.4 and loss tangent 0.02. The designed structure consists of half ring-shaped radiating patch and partial rectangular ground plane to improve the operating bandwidth of the antenna. Moreover, two window-shaped microstrip closed ring resonators are loaded at the back plane of the antenna to provide the notched functionality. The first and the second notched bands are obtained at 7.6 and 9.2 GHz, respectively. Hence, it can reject the interference with X-band and aeronautical radio navigation communications. The proposed miniaturized antenna (19×25 mm^2) is fed using a conventional 50-ohm microstrip line. The designed antenna was simulated and analyzed using CST software. Table 1 illustrates the ideal dimensions of the suggested antenna.

Table 1. Structural dimensions of the proposed antenna

Parameter	Value (mm)	Parameter	Value (mm)
W	25	L2	1
L	5	L3	6
Lg	2.9	L4	3.7
Wf	6.6	R3	0.8
R1	4.5	R4	1.7
R2	2	d1	4
		d2	1.8

3. STRUCTURAL ANALYSIS OF THE ANTENNA

3.1. Structure of UWB antenna

The design steps of the UWB microstrip monopole antenna are illustrated in Figure 2. Figure 3 (a) shows the simulated S_{11} parameter vs. frequency of the designed antenna for different cases of evolution. Firstly, the designed antenna is constructed using the combination of a semi-circular patch and a partial ground

plane to obtain wider operating impedance bandwidth as shown in Figure 2 (case I). It is observed from Figure 3 (a) (case I) that this design combination of the antenna covers the frequency range from (3.0-9.8 GHz) which didn't satisfy the bandwidth requirements of UWB communications. However, by inserting a small circular shape as defected microstrip structure (DMS) in the center of the radiating semi-circular patch as shown in Figure 2 (case II), the bandwidth of the designed antenna was extended by 700 MHz and the operating bandwidth ranges from 3.1 to 10.6 GHz [see Figure 3 (a) (case II)], which can satisfy the frequency range required for UWB systems. The comparison of simulated gains for different design cases are shown in Figure 3 (b). As observed, there are slight variations in gain values at the higher frequencies due to the modifications in the antenna structure as depicted in different design cases. The comparison between bandwidth and fractional bandwidth (%) for the two cases of the design geometry is listed in Table 2.

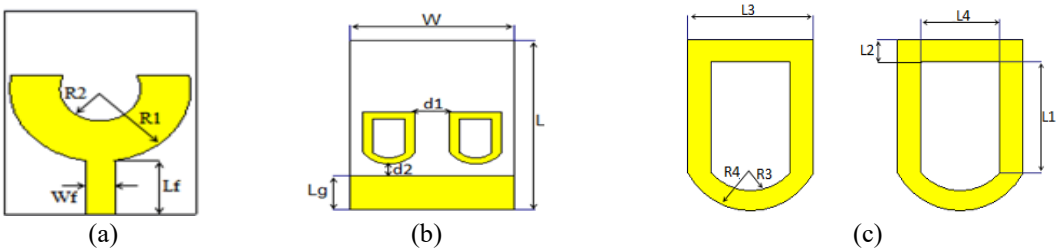

Figure 1. Structure of the proposed UWB antenna; (a) front side, (b) back side, (c) band notch structure

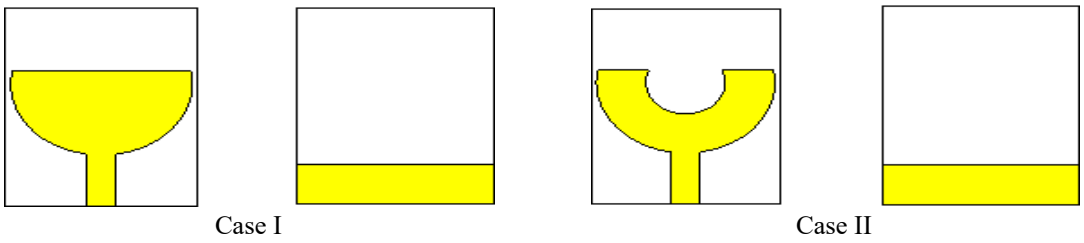

Figure 2. The evolution process of the proposed UWB antenna design

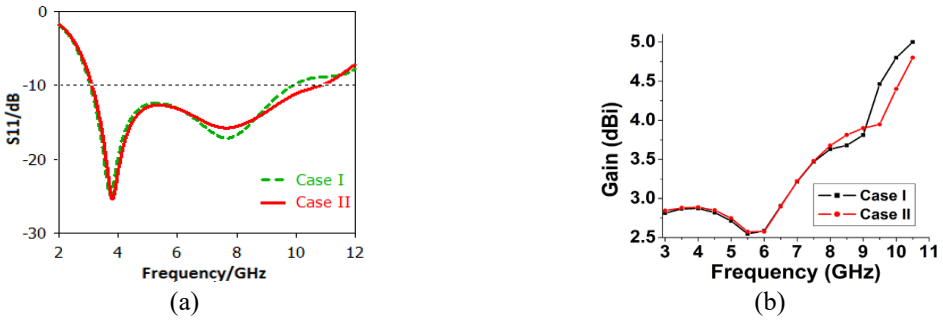

Figure 3. (a). S_{11} parameters for different design steps, (b) gain comparison for different design steps

Table 2. Comparison of operating bandwidths for different design cases

Cases	−10 dB impedance bandwidth	Bandwidth (%)
Case I	3-9.8	106.2
Case II	3.1-10.6	108.4

3.1.1. Structure of UWB notched antenna

Many wireless communication networks such as X-band communication and aeronautical radio navigation systems share the same frequency spectrum (3.1 to 10.6 GHz) along with UWB systems. This common interaction of the frequency spectrum creates interference problems for UWB systems with other

wireless systems. To avoid this problem for a certain frequency band, a novel band rejection technique is presented. This technique consists of an implementation of double microstrip closed ring resonators at the back side of the proposed antenna without altering the dimensional parameters of the basic antenna structure. As the first order of estimations, the total length of the vertical arms of the resonators can be chosen as half of the guided wavelength by the following equation [35]:

$$L_{tot} = \frac{\lambda g}{2} = \frac{c}{2*fnotch*\sqrt{\epsilon eff}} \quad (1)$$

$$\text{where, } \mathcal{E}_{eff} = \frac{\epsilon r+1}{2} \quad (2)$$

Figure 4 shows the design evaluations of the suggested UWB antenna with dual band rejection capability. The corresponding values of simulated S_{11} parameter and voltage standing wave ratio (VSWR) for different design steps of the designed structure are highlighted in Figure 5. As noticed from Figure 4 (case I), the presented structure provides a wide frequency band range which is sufficient to cover the bandwidth requirements of UWB applications. However, it is observed from Figure 4 (case II) that the incorporation of first closed microstrip ring resonator creates a single notch band but the rejection level is not satisfactory in terms of S_{11} level. The appearance of the dual band notches is very prominent due to the incorporation of the second closed microstrip ring resonator [Figure 4 (case III)]. By properly adjusting the dimensions of these rings, the first band notched is centered at 7.5 GHz with a bandstop range from (6.9-8.0 GHz) to overcome interference with X-band downlink (7.25-7.74 GHz). However, the second notched band is centered at 9.1 GHz with band stop range from (8.7-9.5 GHz) to overcome the interference with aeronautical radio navigation (8.7-9.2GHz).

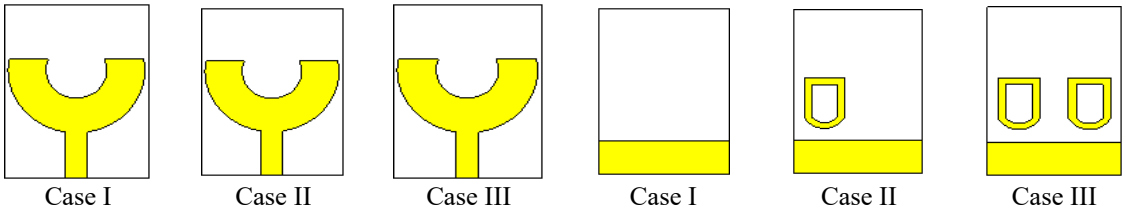

Figure 4. Design evolutions of the proposed UWB antenna

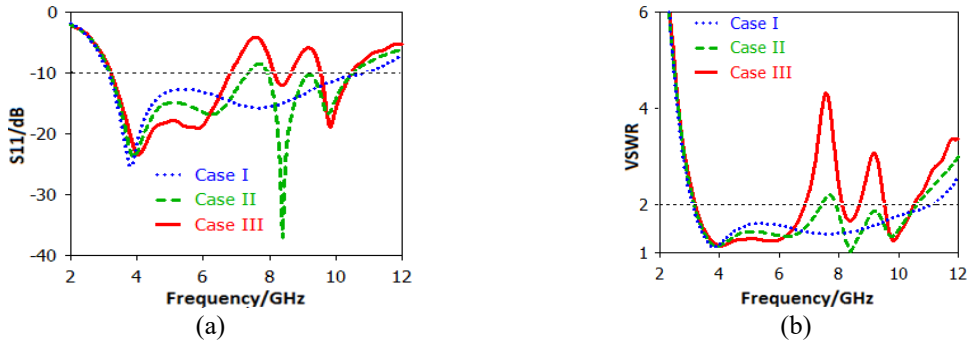

Figure 5. Corresponding values; (a) Simulated S_{11} for different cases, (b) VSWR for different cases

4. PARAMETRIC ANALYSIS

Some parametric experiments have been conducted using CST software to evaluate the features of the antenna and attain the optimum outcome by varying distinct parameters of the antenna.

4.1. Effects of antenna parameter Lg

Figure 6 (a) demonstrates the simulated reflection coefficient response with various Lg values. The length of the ground plane Lg has strong effects on the antenna reflection coefficient. However, the bandwidth and the notched center of the antenna are moderately changed. The optimized value of Lg is 5 mm.

4.2. Effects of antenna parameter L1

The effect of the vertical arms of double microstrip rings, which denoted as L1 are studied. As illustrated in Figure 6 (b), if the value of L1=7 mm, the operating bandwidth of the antenna is decreased by 600 MHz and does not fulfill the bandwidth requirement of UWB applications. Also, there is a prominent shift in the position of the notched bands and the second notch does not support the ARN (8.7 to 9.2 GHz) when designed with L1=7 mm. Similarly, when L1 is changed to 5 mm, the functional bandwidth of the antenna is increased by 400 MHz but the position of the notched bands is shifted in such a way that the intended application bands (7.25 to 7.74 GHz for X-band downlink and 8.7 to 9.2 GHz for ARN) are not covered. The proposed antenna covers the UWB spectrum with dual notching for x band and ARN applications only when designed with L1=6 mm. Hence, the optimized value of L1 is selected as 6 mm for the proposed design.

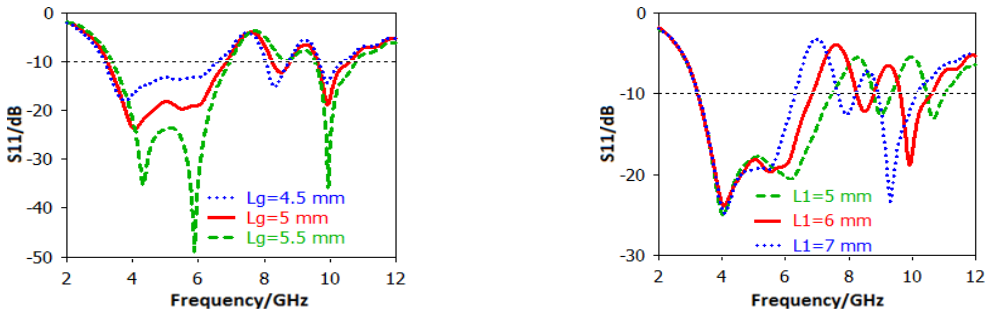

Figure 6. Simulated S_{11} of the proposed antenna; (a) different lengths (Lg) of partial ground, and (b) different lengths of L1

4.3. Effects of antenna parameter L2

The variations of simulated reflection coefficients as a function of L2 are depicted in Figure 7 (a). The operating bandwidth of the antenna remains unaffected with the variations in the dimension of L2. The first notched band is slightly affected. When the structural parameter 'L2' is increased from 1 mm to 2 mm, the center frequency of the first notched band is shifted from 7.6 to 7.8 GHz. The parameter L2 has a significant impact on the second notched band. When L2=1 mm, the second notched band can cover intended ARN applications (8.7-9.2 GHz). Any further change in L2 such as 1.5 mm and 2 mm shifts the position of the second notch band. So, the optimized dimension of L2 is 1 mm.

4.4. Effects of antenna parameter d1

Figure 7 (b) shows the simulated reflection coefficient of the proposed antenna as a function of effective variations in the d1 parameter. When d1 is varied from 2 mm to 6 mm, the position of the second notched band is shifted from 9 to 9.5 GHz, while the position of the first notched band is not affected at all. As noticed from Figure 7 (b), when the distance between the dual rings is decreased, this will increase the coupling effect between the rings, hence this will destroy the second notch completely. The optimized value of d1 is 4 mm.

4.5. Effects of antenna parameter d2

The effective variations of structural parameter d2 have a prominent effect on the resonance characteristics of the proposed antenna as depicted in Figure 8 (a). When d1 is changed from 0.80 to 2.80 mm, the position of the second notch moved from 9 to 9.7 GHz, while the first notched band is slightly moved from 7.4 to 7.6 GHz. However, when d2 is set 0.8mm, this increased the bandwidth and made both notches as a single notch. However, when d2 is set to be 2.80 mm, the second band is slightly disappeared. The optimized value of d2 is considered 1.80 mm.

4.6. Effects of antenna parameter R2

Figure 8 (b) shows the simulated reflection coefficient (S_{11}) vs. frequency plot of the proposed antenna as a function of variations in the design parameter 'R2'. If R2 is increased from 1 mm to 3 mm, the position of the second notched band is moved from 9 GHz to 9.5 GHz, while the first notched band is shifted to 7.8 GHz. However, the operating bandwidth of the suggested antenna remains unaffected.

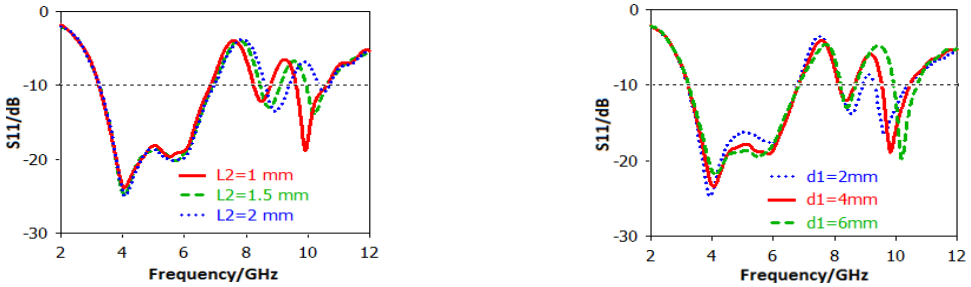

(a) (b)

Figure 7. Simulated S_{11} of the proposed antenna; (a) different lengths of L2, and (b) different lengths of d1

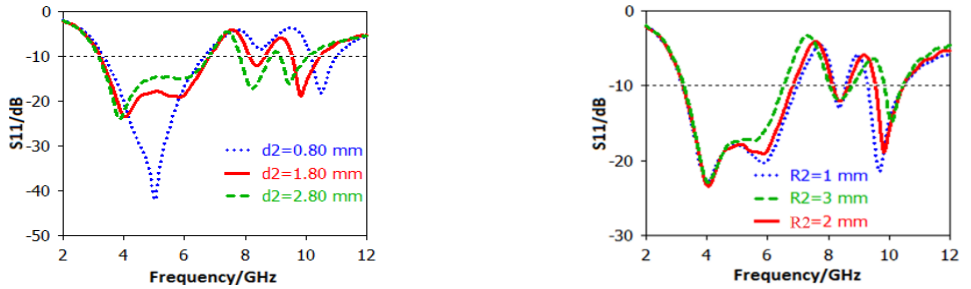

(a) (b)

Figure 8. Simulated S_{11} of the proposed antenna; (a) different lengths of d2, and (b) different lengths of R2

5. CURRENT DISTRIBUTION ANALYSIS

To understand the working mechanism, the surface current distributions of the suggested UWB band-notched antenna are analyzed and presented at the notch frequencies 7.6 and 9.2 GHz, respectively in Figures 9 and 10. The presented figures clarify the dual band-notched feature arising from the band-notch structures. The current density is noted to be heavily localized at the edges of the rings which created the notches. So, from Figures 9 and 10, it can be concluded that the designed antenna shows band rejection characteristics at these frequency bands.

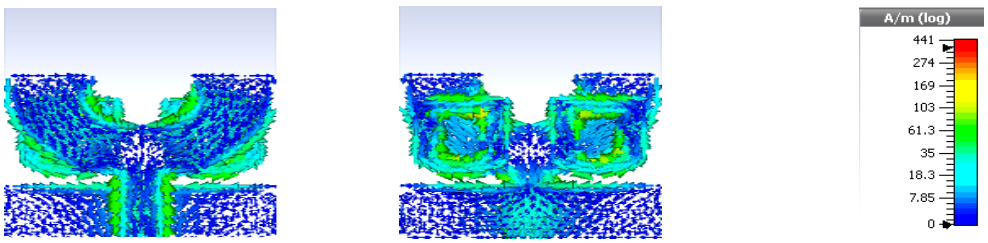

(a) (b)

Figure 9. Surface current distributions of the designed antenna with notch features at 7.6 GHz; (a) front side, and (b) back side

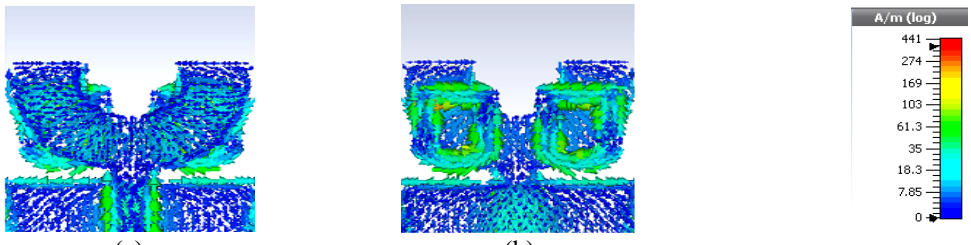

(a) (b)

Figure 10. Surface current distributions of the designed antenna with notch features at 9.2 GHz; (a) front side, and (b) back side

6. RESULTS AND DISCUSSION

The design and simulation study of the proposed antenna has been performed using computer simulation technology (CST) software. The model of the constructed antenna was manufactured and experimentally checked to verify the validity of the proposed antenna model. Figure 11 shows the fabricated structure of the proposed antenna. The simulated (computed by CST software) and measured (using Anritsu MS20038C VNA) reflection coefficients of the proposed antenna is depicted in Figure 12. As presented in Figure 12, the computed and experimental result reveals a very well agreement between them. However, a tiny difference is noted mainly due to the impact of the soldering process of SMA connector and tolerance in the manufacturing process. The measured -10 dB bandwidth of the proposed antenna is extended from 3 to 10.6 GHz to cover most wireless communication applications and UWB communication requirements. It is also observed that the proposed antenna presents an excellent X band downlink rejection band from 7 to 8.1 GHz and ARN rejection band from 8.6 to 9.4 GHz to mitigate the interference with UWB systems. The variation of simulated and measured gains of the proposed antenna (UWB notched band) is depicted in Figure 13. It is noticed from Figure 13 that the peak gain of the antenna reaches 4.53 dBi. However, significant reductions in gain at the notch bands are observed which confirms the band rejection capability of the proposed antenna. The simulated and measured results of the proposed antenna are summarized in Table 3. The co pol components of the E and H plane radiation patterns of the proposed antenna at 3.5 and 5.5 GHz are shown in Figures 14 and 15, respectively.

The cross-polarized components of the fields in E and H planes are shown in Figures 16 (a) and (b). The cross-polarization components at both E and H planes are significantly more than 30 dB down compared to co polarization components. The proposed antenna in the E plane offers almost monopole-like radiation patterns and an acceptable omni-directional H plane radiation patterns for specific frequencies. which indicates efficient transmission of signals by this proposed antenna. The setup used for measurement is shown in Figure 17. The radiation pattern measurement is performed using two antenna measurement process. A standard gain horn on the left side is used as the transmitting antenna and the proposed antenna placed at the right side is used as receiving antenna. The radiation patterns and the gain are measured with turn table mechanism setup and driving software.

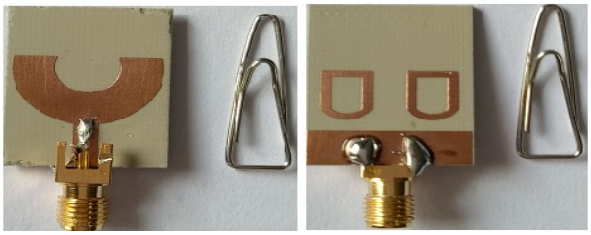

(a) (b)

Figure 11. The fabricated prototype of the proposed antenna; (a) top view (b) bottom view

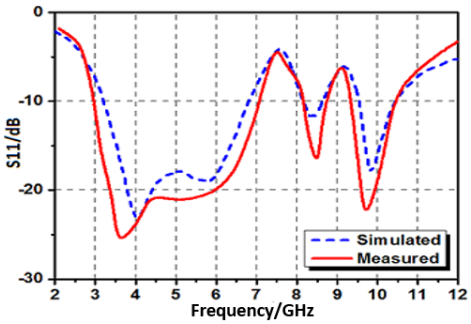

Figure 12. S_{11} parameter of the proposed antenna

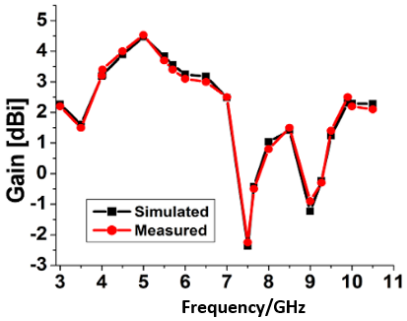

Figure 13. Gain vs. frequency of the proposed antenna

Table 3. Simulated and measured results of the proposed antenna

Proposed Antenna	−10 dB bandwidth (GHz)	Maximum Return loss (dB)	1st notch band (GHz)	2nd notch band (GHz)	Peak gain (dBi)
Simulated	3.15−10.6	23	6.9−8.1	8.5−9.3	4.4
Measured	3−10.6	26	7−8.1	8.6−9.4	4.53

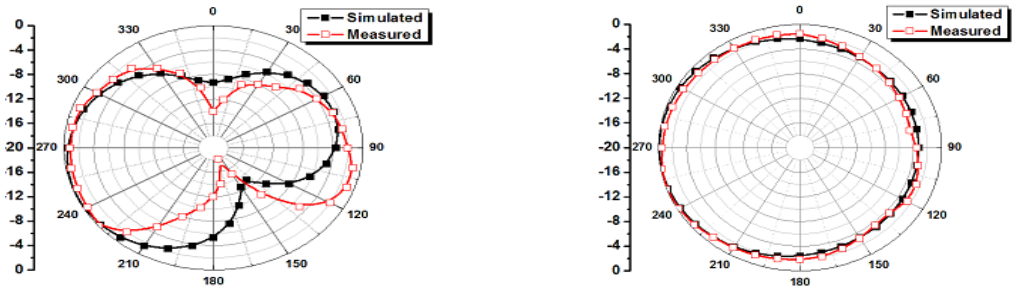

Figure 14. Comparison of simulated and measured radiation patterns at 3.5 GHz;
(a) E-plane and (b) H-plane

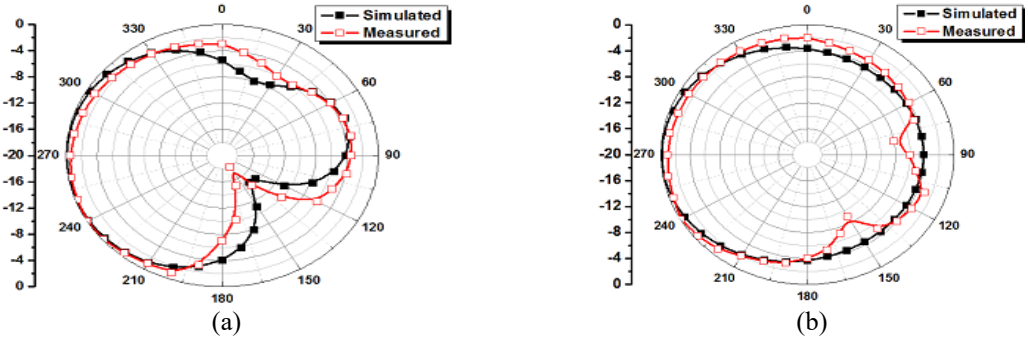

Figure 15. Comparison of simulated and measured radiation patterns (co-pol) at 5.5 GHz;
(a) E-plane and (b) H-plane

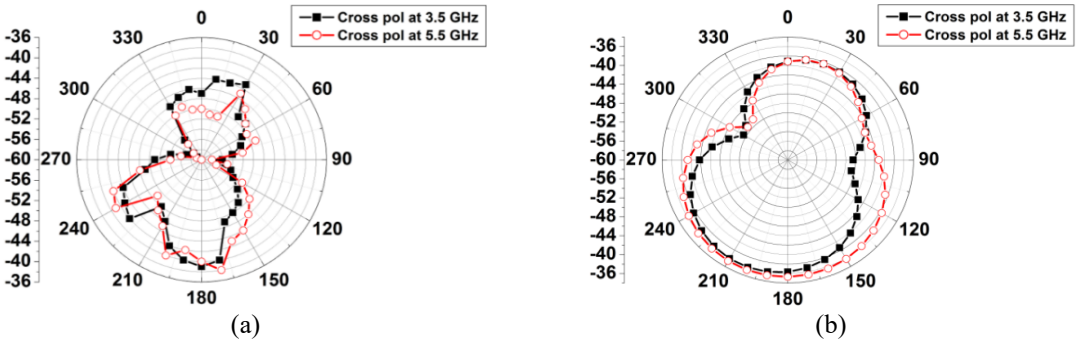

Figure 16. Simulated radiation patterns (cross-pol) at 3.5 GHz and 5.5 GHz; (a) E plane and (b) H plane

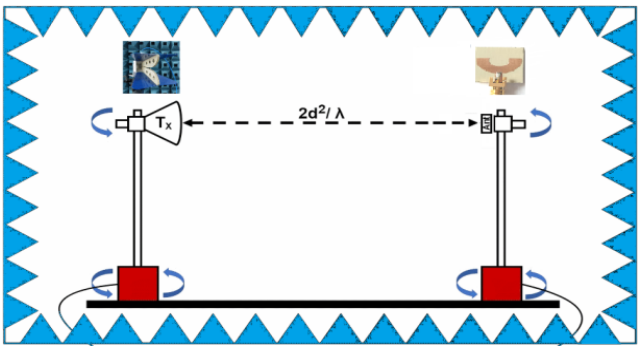

Figure 17. Measurement setup of the proposed antenna

7. PERFORMANCE ANALYSIS OF THE PROPOSED ANTENNA WITH SOME OTHER UWB BAND-NOTCHED ANTENNAS

The characteristic performance comparisons of the suggested antenna with other reported antenna structures [20-33] in respect of dimension, gain and utilization of notch bands are shown in Table 4. A clear conclusion can be drawn from the table that the majority of the recently reported antennas have been designed to provide notch mechanisms for Wi-MAX and WLAN bands. The work presented in this paper has achieved the notch functionality for aeronautical radio navigation as well as X band downlink while keeping a very compact size and well acceptable values of gain. Table 4 shows that the presented antenna is capable to support UWB systems with dual-band rejection functionality for X-band downlink and ARN with the smallest antenna size compared to the other recently reported band-notched UWB antennas.

Table 4. Comparison with reported band-notched UWB antennas

Reference Works	Antenna SizeL×W (mm^2)	Relative permittivity (ε_r)	Peak Gain (dBi)	No. of Notch	Application of Notch band
[20]	32×24	3	4.47	2	WLAN, ITU
[21]	30×20	4.4	4.2	2	Wi-MAX, WLAN
[22]	25×25	4.3	4	2	WLAN, X-band
[23]	41×41	4.4	3.1	2	Wi-MAX, WLAN
[24]	26×27	4.4	4.5	2	Wi-MAX, WLAN
[25]	26×32	4.4	NR	1	WLAN
[26]	33×34	2.2	3.96	2	X-band
[27]	25×25	4.4	3.5	2	Wi-MAX, WLAN
[28]	52×40	2.2	NR	2	Wi-MAX, INSAT
[29]	50×50	2.33	2.1	2	WLAN
[30]	64×50	4.4	NR	1	WLAN
[31]	24.1×21.8	NR	4	2	C-band and X-band
[32]	38×30	4.4	4.5	1	WLAN
[33]	36×36	4.4	3.3	2	LTE, Wi-MAX
Proposed Work	25×19	4.4	4.53	2	X-band downlink, Aeronautical radio navigation (ARN)

NR= Not Reported

8. CONCLUSION

A microstrip line fed compact printed dual band-notched UWB antenna to avoid collision of X-band downlink and aeronautical radio navigation (ARN) with UWB band is discussed. A novel band rejection technique has been implemented on the back side of the proposed antenna to activate band notch features. It has been formed by using a double microstrip ring resonator unit cell. The measured S_{11} parameter demonstrates that the designed antenna has achieved an operating bandwidth ($S_{11} \leq -10$ dB) from 3 GHz to 10.6 GHz, to cover the UWB range, except a notched band 7 to 8.1 GHz (X-band downlink) and 8.6 to 9.4 GHz (aeronautical radio navigation). Furthermore, stable Omni-directional radiation patterns along with significant gains are achieved for the proposed antenna. This suggests that the proposed antenna is suitable for ultra-wideband (UWB) communication system.

REFERENCES

[1] Hertz H., "Electrical Waves," *London, Macmillan and Co*, 1893.
[2] The Federal Communications Commission, "Revision of Part 15 of the Commission's Rules Regarding Ultra Wideband Transmission Systems," 2007.
[3] M. A. Salamin, *et al.*, "Design and realization of low profile dual-wideband monopole antenna incorporating a novel ohm (Ω) shaped DMS and semi-circular DGS for wireless applications," *AEU - International Journal of Electronics and Communications,* vol. 97, pp. 45-53, 2018.
[4] S. Das, *et al.*, "Investigations on miniaturized multifrequency microstrip patch antennas for wireless communication applications," *Journal of Electromagnetic waves and applications,*" vol. 27, no. 9, pp.1145-1162, 2013.
[5] S. Das *et al.*, "Analysis of an open-ended inverted L-shaped slot-loaded microstrip patch antenna for size reduction and multifrequency operation," *Journal of Electromagnetic waves and applications*," vol. 29, no. 7, pp. 874-890, 2015.
[6] M. A. Salamin, *et al.*, "A novel etched-substrate mechanism for characteristics improvement of X band broad band printed monopole antenna," *Microsyst Technol*, 2020.
[7] A. Boutejdar, *et al.*, "A Compact Wideband Monopole Antenna using Single Open Loop Resonator for Wireless Communication Applications," *TELKOMNIKA Telecommunication, Computing, Electronics and Control*, vol. 16, no. 5, pp. 2023-2031, 2018.
[8] S. Das, *et al.*, "Modified π-shaped Slot Loaded Multifrequency Microstrip Antenna," *Progress in Electromagnetics Research B*, vol. 64, no. 1, pp. 103-117, 2015

[9] S. Das, *et al.*, "Analysis of a miniaturized multiresonant wideband slotted microstrip antenna with modified ground plane," *IEEE Antennas and Wireless Propagation Letters,* vol. 14, pp. 60-63, 2015.
[10] A. Boutejder and B. I. Halim, "Analysis and Performance Evaluation of Novel Microstrip Patch Antenna Based on Two Parasitic Ring Resonators and Partial Ground Plane for Multiband Applications," *IEEE International Electromagnetics and antenna conference (IEMANTENNA),* pp. 56-60, 2019.
[11] A. Boutejder and B. I. Halim, "Design of a Compact Tri-band Ring Antenna Using Two Parasitic Ring Resonators and Partial Ground Plane for WiMAX and RADAR Applications", *IEEE International Electromagnetics and antenna conference (IEMANTENNA),* pp. 51-55, 2019.
[12] J. Liang, *et al.*, "Study of a printed circular disc monopole antenna for UWB systems," *IEEE Transactions on Antennas and Propagation,* vol. 53, no. 11, pp. 3500-3504, 2005.
[13] A. M. Abbosh, and M. E. Bialkowski, "Design of ultra wideband planar monopole antennas of circular and elliptical shape," *IEEE Trans. Antennas Propag.* vol. 56, no. 1, pp. 17-23, 2018.
[14] Y. W. Zhong, *et al.*, "Planar circular patch with elliptical slot antenna for ultrawideband communication applications," *Microw Opt Technol Lett.* vol. 57, no. 2, pp.325-328, 2015.
[15] K. Kikuta and A. Hirose, "Compact folded-fin tapered slot antenna for UWB applications," *IEEE Antennas Wirel Propag Lett.,* vol. 14, pp. 1192-1195, 2015.
[16] S. Elajoumi, *et al.*, "Bnadwidth enhancement of compact microstrip rectangular antennas for UWB applications," *TELKOMNIKA Telecommunication, Computing, Electronics and Control,* vol. 17, no. 3, pp. 1559-1568, 2019.
[17] A. El. Hamdouni, *et al.*, "A low cost fractal CPW fed antenna for UWB applications with a circular radiating patch," *TELKOMNIKA Telecommunication, computing, Electronics and control,* vol. 18, no. 1, pp. 436-440, 2020.
[18] A. El. Fatimi, *et al.*, "UWB antenna with circular patch for early breast cancer detection," *TELKOMNIKA Telecommunication, computing, Electronics and control,* vol. 17, no. 5, pp. 2370-2377, 2019.
[19] A. El. Hamdouni, *et al.*, "Novel fractal antenna for UWB applications using the coplanar waveguide feed line," *International Journal of Electrical and Computer Engineering*, vol. 9, no. 4, pp. 3115-3120, 2019.
[20] D. Yadav, *et al.*, "A Compact Dual Band-Notched UWB Circular Monopole Antenna with Parasitic Resonators," *Int. J. Electron. Commun (AEÜ)*., vol. 84, pp.313-320,2018.
[21] J. Malik, *et al.*, "Transient response of dual-band notched ultra-wideband antenna," *International Journal of Microwave and Wireless Technologies,* vol. 7, no. 01, pp.61-67, 2016.
[22] A. H. Majeed, and K. H. Sayidmarie, "UWB elliptical patch monopole antenna with dual band notched characteristic," *International Journal of Electrical and Computer Engineering,* vol. 9, no. 5, pp. 3591-3598, 2019.
[23] G. Srivastava, and B. K. Kanuijia, "Compact dual band-notched UWB MIMO antenna with shared radiator," *Microwave and Optical Technology Letters,* vol. 57, no. 12, pp. 2886-2891, 2015.
[24] A. P. Singh *et al.*, "UWB antenna with dual notched band for WiMAX and WLAN applications," Microwave *and Opt. Technol. Lett.,* vol. 59, no. 4, pp. 792-797, 2017.
[25] O. Kumara, and S. Soni, "Design and analysis of Ultra-wideband microstrip patch antenna with notch band characteristics," *MATEC Web of Conferences 57*, 2016.
[26] A. Iqbal, O. A. Saraereh, and S. K. Jaiswal, "Maple Leaf Shaped UWB Monopole Antenna with Dual Band Notch Functionality," *Progress in Electromagnetics Research C*, vol. 71, pp. 169-175, 2017.
[27] Y. Zehforoosh, and T. Sedghi, "An improved CPW fed printed UWB antenna with controllable band notched functions," *Journal of Communication Engineering,* vol. 5, pp. 38-49, 2016.
[28] S. Peddakrishna, and T. Khan, "Design of UWB Monopole Antenna with Dual Notched Band Characteristics by Using π-Shaped Slot and EBG Resonator," *AEU - International Journal of Electronics and Communications,* vol. 96, pp.107-112, 2018.
[29] H. Peng, *et al.*, "Novel SRR-loaded CPW-fed UWB antenna with wide band-notched characteristics*," International Journal of Microwave and Wireless Technologies*. vol. 9, no. 4, pp.875-880, 2017.
[30] G. S. Rao, *et al.*, "Cross shaped slot printed UWB monopole antenna with notch function," *Microsystem Technologies,* vol. 21, no. 11, pp. 2327-2330, 2015.
[31] S. K. Vijay, *et al.*, "UWB antenna with dual band notch," *International Journal of Engineering and Advanced Technology,* vol. 8, pp. 61-65, 2019.
[32] R. Labade, *et al.*, "Compact integrated Bluetooth UWB band notch antenna for personal wireless communication," *Microwave and Opt. Technol. Lett.,* vol. 58, no. 3, pp. 540-546, 2016.
[33] S. C. Puri, *et al.*, "An UWB trapezoidal rings fractal monopole antenna with dual-notch characteristics," *International Journal of RF and Microwave Computer-Aided Engineering,* vol. 29, no. 8, 2019.
[34] S. Lakrit, *et al.*, "A compact UWB monopole patch antenna with reconfigurable Band-notched characteristics for Wi-MAX and WLAN applications," *AEU - International Journal of Electronics and Communications,* vol. 105, pp.106-115, 2019.
[35] M.A. Salamin, *et al.*, "A novel UWB antenna using capacitively-loaded fork-shaped resonator and modified fork-shaped DMS for interference mitigation with WiMAX and WLAN applications," *Journal of Instrumentation,* vol. 14*,* 2019.